IEEE Access
Multidisciplinary | Rapid Review | Open Access Journal

Received 27 June 2025, accepted 27 July 2025, date of publication 30 July 2025, date of current version 8 August 2025.

Digital Object Identifier 10.1109/ACCESS.2025.3593996

RESEARCH ARTICLE

A Novel Hybrid Analysis Method of LLC Resonant Converter for High Accuracy and Low Computational Burden

SU-SEONG PARK AND RAE-YOUNG KIM, (Senior Member, IEEE)
Department of Electrical and Biomedical Engineering, Hanyang University, Seoul 04763, South Korea

Corresponding author: Rae-Young Kim (rykim@hanyang.ac.kr)

This work was supported by the National Research Foundation of Korea (NRF) grant funded by Korean Government (MSIT) under Grant 202400000003005.

ABSTRACT Recently, as the demand for LLC resonant converters has increased in various power electronics industry sectors, research on accurate analysis methods necessary for effectively designing converters has been conducted. This paper proposes an analysis model that can estimate the efficiency of the converter and the temperature of component parts with high accuracy while requiring a relatively low computational burden when analyzing LLC resonant converters. The proposed analysis model performs circuit and thermal analysis using advanced mathematical modeling methods based on time analysis, and uses a hybrid structure analysis model that analyzes magnetic components through an AI-based analysis model. Time analysis-based analysis is a method that accurately estimates the magnitude of voltage and current of resonant converters by equivalent modeling of circuit configurations for each operating state during a switching cycle using nonlinear circuit equations. The AI-based analysis model is a method that generates the relationship between design input variables and output variables of magnetic components through AI algorithms and uses this as an analysis model. To verify the effectiveness of the proposed method, a 1kW LLC resonant converter prototype is used, and the efficiency and temperature estimation accuracy of the proposed method are measured under various capacity conditions, input and output voltage conditions, resonant network conditions, and load conditions. The proposed method estimates efficiency with an error within 2% and estimates temperature with an error within 10% under various verification conditions. In terms of computation time, it takes about 7000[s] for 100 analyses, which shows relatively low computational burden compared to existing methods. Through this, the proposed method can effectively analyze LLC resonant converters with high accuracy and relatively low computational burden.

INDEX TERMS LLC resonant converter, time domain analysis, thermal impedance modeling, surrogate model, GaN switch, estimation error, computational burden.

I. INTRODUCTION

Recently, there has been an increasing demand for DC-DC power conversion devices using power semiconductor switches in various power electronics industry sectors such as fuel cell power converters, server modules, and photovoltaic systems [1], [2], [3]. In particular, the LLC resonant converter, one of the widely used DC-DC power conversion devices, allows soft switching within the operating frequency condition, making it easy to achieve high efficiency. It also enables high-density power converter design

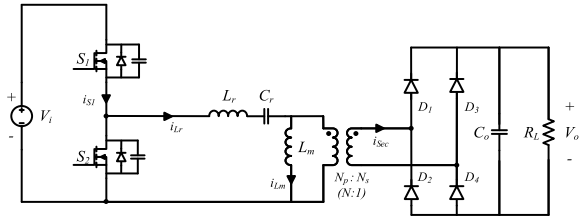

FIGURE 1. LLC resonant converter.

The associate editor coordinating the review of this manuscript and approving it for publication was Khaled Ahmed.

TABLE 1. Literature review of previous research about analysis model of LLC resonant converter.

	Equation based Analysis Model (Ref [15]-[25])		Simluation based Analysis Model (Ref [26]-[31])		AI based Analysis Model (Ref [32]-[35])	
	Circuit	Magnetic	Circuit	Magnetic	Circuit	Magnetic
Accuracy	Medium (TDA : Relatively High)	Low	High	High	Relatively High	Relatively High
Computation Burden	Low	Low	High	High	Medium	Medium
Complexity	Low	Low	High	High	Medium	Medium

by reducing the size of passive components in the power conversion device through high-frequency operation [4], [5], [6]. As shown in Figure 1, an LLC resonant converter consists of various components including power switches, diodes, resonant inductors, resonant capacitors, transformers, and output capacitors, and can be designed by selecting appropriate components according to design specifications [7], [8]. For designing high-efficiency, high-density LLC resonant converters, a technique that can accurately analyze the LLC resonant converter circuit is necessary, and a comprehensive analysis method that can consider the physical and electrical characteristics of converter components based on this is required [9], [10].

Generally, LLC resonant converters operate using the resonant phenomenon of inductors, transformers, and capacitors in the primary circuit, and the operating currents and voltages in the circuit have nonlinear characteristics, making accurate circuit analysis difficult [11], [12]. Additionally, among the components constituting the LLC resonant converter, inductors and transformers have various design and analysis variables compared to other components, and accurate analysis is difficult due to the nonlinear characteristics of the analysis results [13], [14]. Therefore, various techniques have been researched for accurate circuit and magnetic analysis of LLC resonant converters [15], [16], [17], [18], [19], [20], [21], [22], [23], [24], [25], [26], [27], [28], [29], [30], [31], [32], [33], [34], [35].

References [15], [16], [17], [18], [19], [20], [21], and [22] are techniques for analyzing the circuit and magnetic components of LLC resonant converters through mathematical modeling-based analysis formulas. These techniques analyze the physical and electrical characteristics of circuits and magnetic components through formulas composed of variables for converter design and analysis. They derive result values based on key variables through the analytical formulas, providing the advantage of intuitive and simple analysis of circuits and passive components. However, for components such as magnetic elements that require consideration of many design and analysis variables, and where the causality of analysis results according to variables is not clear, the accuracy compared to actual values is found to be not high. For more specific research on mathematical modeling-based analysis formulas, [15], [16], [17], [18], [19] proposed methods for analyzing LLC resonant converters using mathematical modeling-based analysis formulas. [15], [16] analyzed the circuit of LLC resonant converters through frequency-based analysis formulas. While these have the advantage of allowing simple and intuitive analysis of LLC resonant converters through frequency-based analysis formulas, they have limitations in that they cannot fully reflect the characteristics of harmonic components existing in the circuit, resulting in low analysis accuracy depending on frequency and load conditions. References [17], [18], and [19] proposed methods to analyze LLC resonant converters based on the time domain to compensate for such disadvantages. Unlike frequency-based analysis formulas that do not consider harmonic components or analyze them briefly, these methods can perform accurate analysis according to the operating conditions of LLC resonant converters through nonlinear analysis formulas based on the time domain. References [20], [21], and [22] are methods for analyzing the magnetic components of converters through mathematical modeling-based analysis formulas. By gradually developing the basic Steinmetz equation, the formulas are structured to consider more complex magnetic component design and analysis variables, and converter operating conditions [20]. While there is an advantage in that analysis can be performed through simple formulas with clear causality between variables and analysis results, it is difficult to guarantee accurate magnetic analysis results in various operating environments [22].

References [23], [24], and [25] proposed methods for analyzing LLC resonant converter circuits and analyzing magnetic components using circuit and magnetic analysis simulation-based analysis techniques. The proposed methods analyze the converter's circuit and magnetic components using simulation tools, providing the advantages of high accuracy compared to actual result values and broad consideration of various variables [23]. However, they have limitations in that they require specialized knowledge of professional simulation tools for analysis, and the computational burden required for the technique is relatively large compared to other techniques. References [26], [27],

and [28] are methods for performing circuit and magnetic analysis through AI-based analysis models. These techniques involve deriving a representative analysis model that can represent the nonlinearity between design and analysis variables and result values by training simulation and experimental data using AI algorithms, and performing analysis through this. These techniques have the advantage of deriving analysis result values with relatively high accuracy in systems with nonlinearity that need to consider various design variables. They have a larger computational burden than mathematical modeling-based analysis formulas but a smaller computational burden than simulation-based analysis techniques. AI-based representative models, once trained, function as black-box models that can produce high-accuracy results—such as efficiency, temperature, and volume—by simply inputting analysis parameters. Since this approach does not require in-depth operation of simulation tools, it is considered relatively simple, provided that the user is familiar with how to prepare and apply input parameters appropriately. In conclusion, by combining mathematical modeling-based analysis and AI-based analysis minimizes overall analysis complexity by utilizing a time-domain mathematical model (TDA) for circuit analysis and an AI-based model for magnetic component analysis. Compared to other approaches—such as using simulation-based methods for both circuit and magnetic analysis, or applying mathematical modeling only for circuit analysis while relying on simulation for magnetic components—the proposed hybrid method offers a relatively simple and efficient alternative. Table 1 summarizes the characteristics of the previously proposed analysis techniques in terms of estimation accuracy, computational burden, and technique complexity.

This paper proposes an analysis model that can estimate the efficiency and temperature of the converter with high accuracy and does not require a large computational burden when analyzing LLC resonant converters. The proposed analysis model is a technique that has relatively high estimation accuracy and relatively low computational burden in circuit, thermal, and magnetic analysis by combining an advanced mathematical modeling analysis model based on time analysis and an AI-based analysis model. The proposed method is verified through LLC resonant converters under various operating and design conditions, and the effectiveness of the proposed method is verified through performance comparison with conventional methods.

II. CONVENTIONAL ANALYSIS METHODS OF LLC RESONANT CONVERTER

A. CONVENTIONAL EQUATION BASED ANALYSIS MODEL

One of the representative methods for analyzing the circuit of LLC resonant converters through mathematical modeling-based analysis formulas is the frequency-based analysis method, which analyzes LLC resonant converters relatively simply without considering all harmonic components [16]. As shown in Fig. 1, an LLC resonant converter can be configured with switches ($S_1 \sim S_2$) and diodes ($D_1 \sim D_4$) in the secondary side. V_i and V_o represent the input and output voltages, and R represents the load resistance. The resonant network constituting the primary circuit consists of resonant inductance L_r, resonant capacitor C_r, and the magnetizing inductance L_m of the high-frequency transformer. The number of turns of the primary side of the high-frequency transformer is represented as N_p, the number of turns of the secondary side as N_s, and the turns ratio can be represented as N ($= N_p/N_s$). In Fig. 1, the primary side switch circuit is equivalently transformed into a sinusoidal voltage source V_{AB}, and the equivalent resistance R_{ac}, which is the secondary side rectifier circuit and load transformed to the primary side of the high-frequency transformer, can be represented. From this, an equivalent circuit of the LLC resonant converter as shown in Fig. 2 can be derived. The output terminal voltage V_{AB} of the primary side switch circuit can be expressed as (1), where the variable t is time, n is the harmonic order, and w_s is the switching frequency. In the case of the FHA technique, since only the fundamental component is considered, the voltage defined as $V_{AB,1}$ by applying the condition $n=1$ to the (2) of the input square wave component is expressed as (3). When the voltage across R_{ac} in Fig. 2 is defined as V_{eq}, the output voltage can be obtained through the voltage division law according to the impedance magnitude ratio that changes with frequency, as shown in (4). Through this, the output voltage magnitude ratio according to the input voltage can be derived, which can be considered as one of the important parameters in converter design [29].

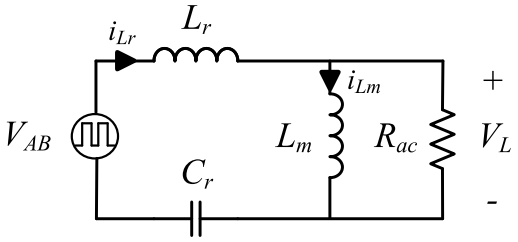

FIGURE 2. Equivalent model of LLC resonant converter for frequency domain analysis.

$$V_{AB}(t) = \sum_{n=1,3,5\cdots}^{\infty} V_{AB\_n}(t) \tag{1}$$

$$V_{AB\_n}(t) = \frac{4 \cdot V_{in}}{\pi} \cdot \frac{1}{n} \sin(nw_s t) \tag{2}$$

$$V_{AB\_1} = \frac{4 \cdot V_{in} \cdot \sin(w_s)}{\pi} \tag{3}$$

$$V_L = V_{AB\_1} \frac{jwL_m // R_{ac}}{jwL_m + jwL_m // R_{ac} + 1/jwC_r} \tag{4}$$

A representative method for analyzing magnetic components in LLC resonant converters through mathematical modeling-based analysis formulas is the Steinmetz method, which can be expressed as (5) [30]. ΔB represents the

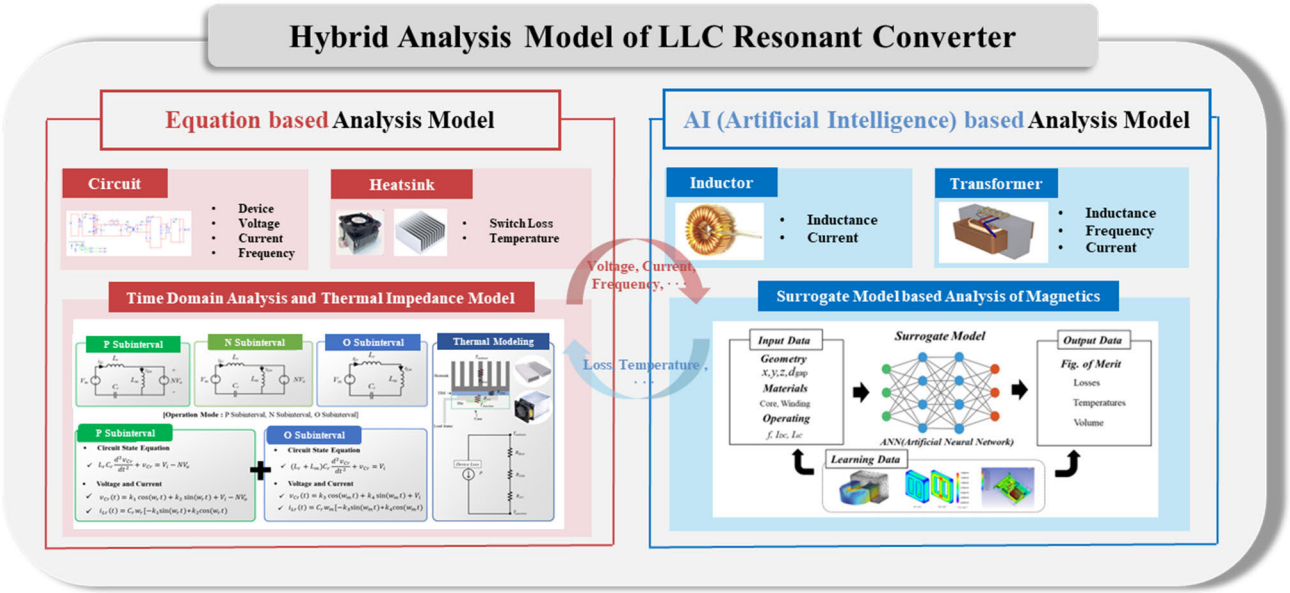

FIGURE 3. Proposed hybrid analysis model for LLC resonant converter.

magnitude of the average flux density in a frequency-based sinusoidal system, P_v represents the magnitude of the loss of the magnetic material per unit volume, and k, α, β are coefficients according to the core type and material of the magnetic component.

$$P_v = kf^{\alpha}(\Delta B)^{\beta} \tag{5}$$

The basic Steinmetz equation has the limitation that the accuracy of analysis decreases when based on waveforms with different forms such as square waves, as it is analyzed based on ideal sinusoidal waves. Several approaches have been developed to cover this disadvantage. As analyzed in [31], [32], and [33], a modified Steinmetz equation was proposed based on the fact that P_v directly depends on dB/dt. In particular, [32], [33] analyzed parameters in the magnetic hysteresis loop that directly affect the magnitude of P_v and presented a method that can accurately derive the magnitude of P_v. Through this, a generalized Steinmetz equation (iGSE) was derived, which can be expressed as (6)-(7).

$$P_v = \frac{1}{T}\int_0^T k\left|\frac{dB}{dt}\right|^{\alpha}(\Delta B)^{\beta-\alpha}dt \tag{6}$$

$$k_i = \frac{k}{(2\pi)^{\alpha-1}\int_0^{2\pi}|\cos\theta|^{\alpha}\,2^{\beta-\alpha}d\theta} \tag{7}$$

The method for analyzing the temperature of magnetic components based on mathematical modeling is expressed as (8) [34]. Here, ΔT_{rise} represents the magnitude of temperature rise, P_t represents the magnitude of magnetic loss, which is the sum of core loss and copper loss, and A_{sf} represents the sum of the surface area of the magnetic component. The relationship between the temperature rise rate value according to the loss and the sum of the surface area obtained under various shapes and design conditions of magnetic components is represented in (8). The experimental input and output result values was related with an exponential function form of formula and proportional constant, which can be used to estimate the temperature of the core and winding of magnetic components under various design conditions.

$$\Delta T_{rise} = 450 \times \left(\frac{P_t}{A_{sf}} \times 10^{-4}\right)^{0.826} \tag{8}$$

The method of estimating the temperature of magnetic components through mathematical modeling has the advantage of easily obtaining values through a simple formula form, but it has many limitations in terms of estimation accuracy as the variables considered are limited.

B. CONVENTIONAL SIMULATION BASED ANALYSIS MODEL

This is a method of analyzing the circuit and magnetic component elements of LLC resonant converters through dedicated circuit and magnetic analysis simulations. When using circuit analysis simulation, the circuit constants and design specifications of the LLC resonant converter are inputted, and through dedicated circuit simulation, losses, temperature according to thermal resistance reflection, etc., can be calculated. In the case of magnetic analysis simulation, variables constituting the magnetic components and the finite element method are used to solve Maxwell's equations to calculate the distribution of electric field E and magnetic field H respectively, and based on this, values

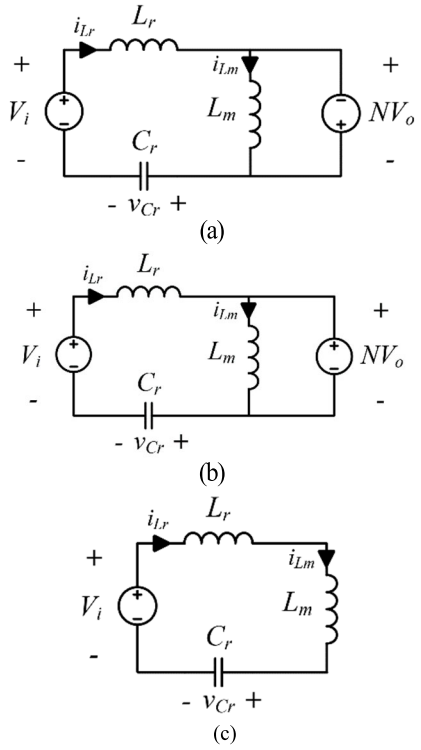

FIGURE 4. Equivalent circuit of the resonant converter at different subintervals (a) P subinterval (b) O subinterval (c) N subinterval.

such as loss and temperature of the magnetic components can be obtained. In the case of this simulation, the result values vary greatly depending on the structure, shape, size of the magnetic component, and the size and number of mesh, which is the analysis unit [35]. When using magnetic analysis simulation, various variables required for design and analysis can be considered comprehensively, and through this, accurate physical and electrical analysis results can be obtained. However, expertise is required to derive reliable results in using the simulation, and to derive accurate circuit and magnetic analysis results, the computation time takes from a few minutes to as long as several days [36]. This has the limitation of restricting the number of analyses that can be performed in situations where various analyses need to be considered.

III. PROPOSED HYBRID ANALYSIS MODEL OF LLC RESONANT CONVERTER

The proposed hybrid analysis model of LLC resonant converter consists of a combination of two analysis models. It uses advanced mathematical modeling-based analysis formulas for circuit and thermal analysis, and for magnetic analysis, it estimates the magnitude of loss and temperature of magnetic components through an AI-based analysis model. Both analysis models can accurately estimate the efficiency and temperature of the components of the LLC resonant converter, and the computational burden required for analysis is not large, making it an effective technique for analyzing LLC resonant converters. Fig. 3 shows the overall structure of the proposed hybrid analysis model. The mathematical modeling-based analysis formula is used for circuit and thermal analysis of switches and diodes, and through an advanced analysis formula, the time analysis-based LLC resonant converter analysis technique and thermal impedance-based modeling can accurately determine the magnitude of voltage and current in the circuit, and through this, the loss of switches and diodes can be derived. Additionally, the heat sink for switches and diodes can be selected through the obtained loss and thermal impedance modeling, and through this, the temperature of switches and diodes can be estimated. Information about operating conditions such as voltage, current, frequency, etc., derived through TDA is transmitted to the magnetic analysis model and used in magnetic analysis. The AI-based analysis model is an analysis method that establishes the relationship between input and output design and analysis variables of magnetic components through a deep learning-based representative model, which has better accuracy than mathematical modeling-based relationship formulas and shorter computation time than simulation-based analysis. The time-domain modeling approach enables precise analysis of the nonlinear voltage and current waveforms that occur during the converter's operation. Unlike frequency-domain methods that have limitations in capturing harmonic components, the proposed time-domain model provides more accurate estimation of the actual voltage and current magnitudes. Based on this, the method allows for reliable estimation of power loss and efficiency.

In addition, the AI-based model effectively captures complex and nonlinear relationships between design variables and output characteristics (e.g., efficiency and temperature) by learning from simulation and experimental data. This data-driven approach allows the model to reflect implicit behaviors that are difficult to express explicitly through conventional mathematical formulas. The combination of these two techniques enhances the overall estimation accuracy. In LLC resonant converters where circuit, thermal, and magnetic characteristics interact in complex ways, the proposed method achieves higher precision compared to conventional techniques. Through this analysis model, the core loss, copper loss, and temperature of magnetic components can be derived. By combining the information of the circuit analysis model based on mathematical modeling and the magnetic analysis model based on AI, a comprehensive analysis of the efficiency, volume, and temperature of the LLC resonant converter can be performed.

A. DESIGN METHOD OF THE PROPOSED CONTROL TECHNIQUE

The mathematical modeling-based analysis technique mainly performs circuit and thermal analysis and consists of the TDA technique, which analyzes LLC resonant converters based on the time domain, and thermal impedance modeling. Fig. 5 shows the mathematical modeling-based analysis

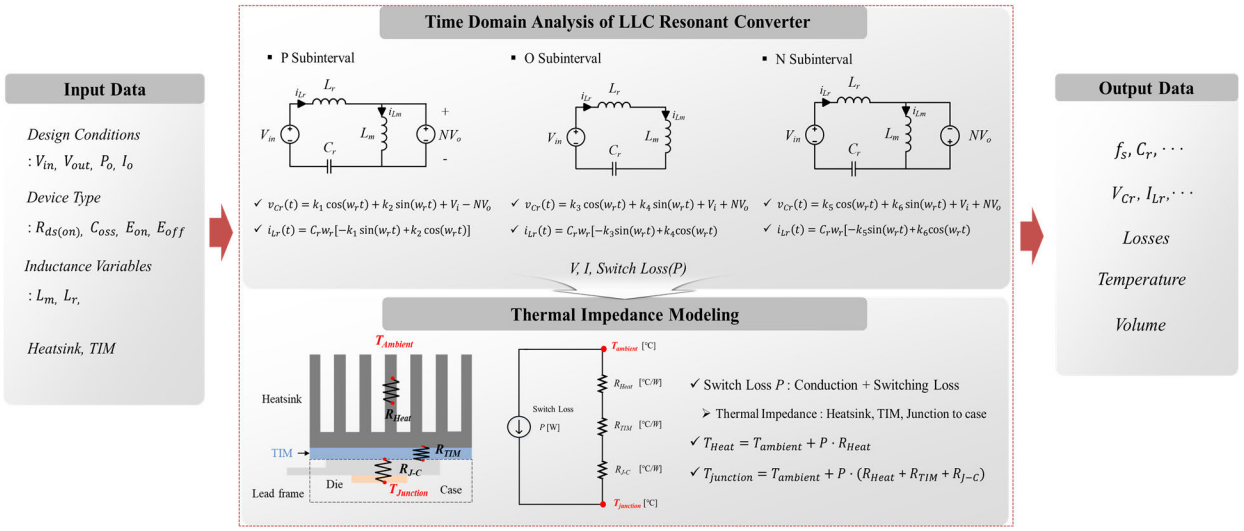

FIGURE 5. Equation based Analysis Model for LLC resonant converter.

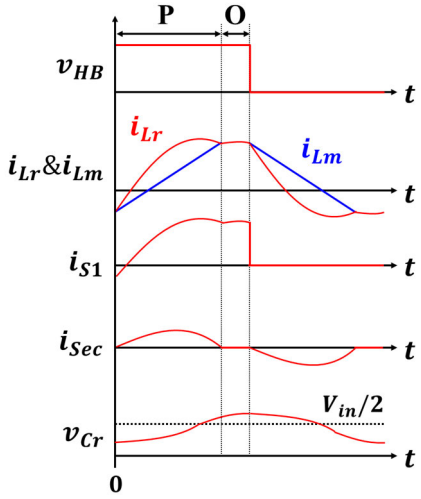

FIGURE 6. Operation waveforms in PO operation mode.

technique, with input data including input and output voltages V_{in}, V_{out}, capacity P_o, output current I_o, device data such as on-resistance $R_{ds(on)}$, switch output capacitance C_{oss},, and switch turn-on and turn-off energies E_{on},E_{off}. Operating conditions and related variables to consider include switching frequency f_s, resonant frequency f_r, magnetizing inductance L_m, resonant inductance L_r, resonant capacitance C_r etc. and also include the type of heat sink and TIM material. By inputting the input data into the proposed mathematical modeling-based analysis model, information about the operating conditions of the LLC resonant converter such as voltage, current, and switching frequency can be obtained, and information about the loss, temperature, and volume of switches and diodes, including the heat sink, can be obtained.

1) TDA(TIME DOMAIN ANALYSIS)

TDA (Time Domain Analysis) derives nonlinear circuit equations by equivalently transforming the circuit configuration for each operating state during a converter's switching cycle. Through the method of deriving time-domain solutions for resonant network voltage and current, it has the advantage of analyzing the circuit with high accuracy under various operating frequencies and load conditions [37]. Fig. 4 shows the circuit configuration for each operating state during a switching cycle of the LLC converter. The P interval in Figure 4 (a) is the case where the voltage across the magnetizing inductor L_m of the LLC resonant converter is clamped to the positive output voltage NV_O, and when Kirchhoff's voltage law (KVL) is applied to the equivalent circuit of the P interval, it is expressed as a differential equation as shown in Equation (9).

$$L_r C_r \frac{d^2}{dt^2} v_{Cr} + v_{Cr} = V_i - NV_O \tag{9}$$

When finding the general solution of (9), it can be expressed as the C_r voltage as shown in (10) and the L_r current as shown in (11). Here, k_1,k_2 are coefficients determined by the initial conditions of the circuit, and the series resonant angular frequency w_r can be defined as shown in (12).

$$v_{Cr}(t) = k_1 cos\,(w_r t) + k_2 sin\,(w_r t) + V_i - NV_o \tag{10}$$

$$i_{Lr}(t) = C_r w_r[-k_1 sin\,(w_r t) + k_2 cos\,(w_r t)] \tag{11}$$

$$w_r = \frac{1}{\sqrt{L_r C_r}} \tag{12}$$

The N interval in Fig. 4 (b) is the case where the voltage across the magnetizing inductor L_m is clamped to the negative output voltage -NV_O, and when Kirchhoff's voltage law (KVL) is applied to the equivalent circuit of the N interval,

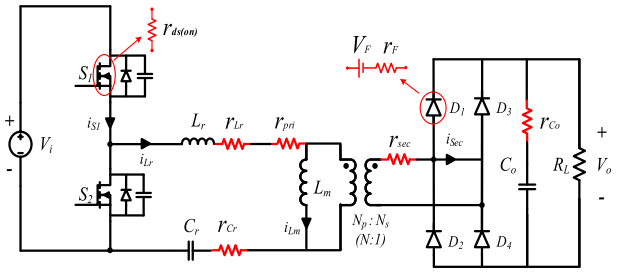

FIGURE 7. Thermal impedance structure and circuit of LLC Resonant converter (a) Thermal impedance structure (b) Thermal impedance circuit.

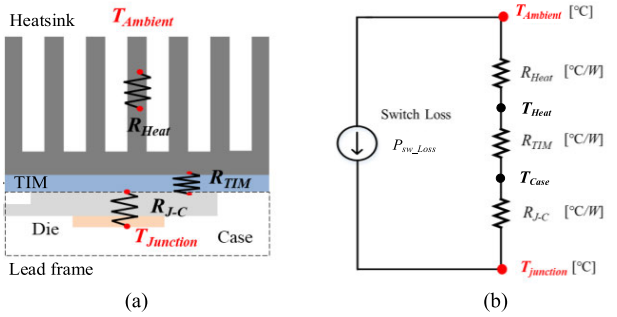

FIGURE 8. Resistance model of LLC resonant converter for conduction loss.

it is expressed as (13).

$$L_r C_r \frac{d^2}{dt^2} v_{Cr} + v_{Cr} = V_i + NV_O \tag{13}$$

When finding the general solution of (13), it can be expressed as (14) and (15) for C_r voltage and L_r current respectively, where k_3, k_4 are coefficients determined by the initial conditions of the N interval circuit.

$$v_{Cr}(t) = k_3 cos\,(w_r t) + k_4 sin\,(w_r t) + V_i + NV_o \tag{14}$$

$$i_{Lr}(t) = C_r w_r [-k_3 sin\,(w_r t) + k_4 cos\,(w_r t)] \tag{15}$$

The O interval in Fig. 4 (c) is the case where the voltage across the magnetizing inductor L_m is not clamped to the output voltage, and the differential equation of the equivalent circuit of the O interval is as shown in (16), and through the general solution, the equations for C_r voltage and L_r current (17)-(18) can be obtained.

$$(L_r + L_m) C_r \frac{d^2}{dt^2} v_{Cr} + v_{Cr} = V_i \tag{16}$$

Here, k_5, k_6 are coefficients determined by the initial conditions of the O interval circuit, and the parallel resonant angular frequency w_m is expressed as (17).

$$v_{Cr}(t) = k_3 cos\,(w_r t) + k_4 sin\,(w_r t) + V_i + NV_o \tag{17}$$

$$i_{Lr}(t) = C_r w_r [-k_3 sin\,(w_r t) + k_4 cos\,(w_r t)] \tag{18}$$

$$w_m = \frac{1}{\sqrt{(L_r + L_m) C_r}} \tag{19}$$

The operating mode of the LLC resonant converter is formed by different combinations of the three intervals defined earlier: P, N, and O. For example, if the half-cycle operation of the LLC resonant converter starts with the P interval and ends with the O interval, it is defined as the PO operating mode, and Fig. 6 shows the current and voltage waveforms in the PO operating mode of the LLC resonant converter. v_{HB} represents the magnitude of the output voltage of the LLC resonant converter pole, and i_{Lr} and i_{Lm} represent the resonant current and magnetizing current, respectively. i_{s1} represents the magnitude of the upper switch current, i_{sec} represents the magnitude of the secondary side rectifier current, and v_{Cr} represents the magnitude of the resonant capacitor voltage. The PO operating mode consists of the P operating mode and O operating mode according to the magnitude of the voltage across the magnetizing inductor, as defined earlier. Generally, the LLC resonant converter can operate in nine main modes: PO, PON, PN, P, O, NP, NOP, OP, and OPO, and the corresponding operating mode differs according to operating conditions such as operating frequency and load magnitude [38]. Therefore, for time-domain-based analysis of LLC resonant converters, criteria for classifying operating modes according to operating conditions are required, and through this, a more accurate LLC resonant converter analysis can be performed [39]. The loss of the LLC resonant converter can be analyzed through the accurately derived voltage and current magnitudes via the TDA technique, and through this, the efficiency magnitude can be calculated. The loss of the LLC resonant converter can be divided into three main categories for analysis. First, for switching loss, assuming that the LLC resonant converter performs ZVS (Zero Voltage Switching) operation due to its characteristics, only the switching loss that occurs when the switch turns off is considered.

$$P_{sw} = 2E_{off}(V_i, I_{s,off}) f_s \tag{20}$$

Here, the turn-off loss can be calculated through the switch's turn-off energy and switching frequency, as shown in (20). E_{off} is the turn-off switching energy, which is a value that changes according to the input voltage V_i and turn-off current $I_{s,off}$ magnitude. The magnitude of the turn-off voltage and turn-off current, which are determined by the operating conditions, can be accurately determined through TDA, and through this, the turn-off switching loss is calculated. Next is the conduction loss of the LLC resonant converter. Fig. 7 shows the circuit with resistance components constituting the conduction loss in the LLC resonant converter circuit. Conduction loss can be divided into conduction loss due to the switch's on-resistance $r_{ds(on)}$, conduction loss due to the parasitic resistance values r_{Cr} and r_{Lr} of C_r and L_r in the resonant network, conduction loss due to the transformer's primary and secondary winding resistance r_{pri}, r_{sec} and conduction loss due to the diode's forward voltage drop V_F and equivalent resistance r_F, and conduction loss due to the parasitic resistance value r_{Co} of the output capacitor C_o.

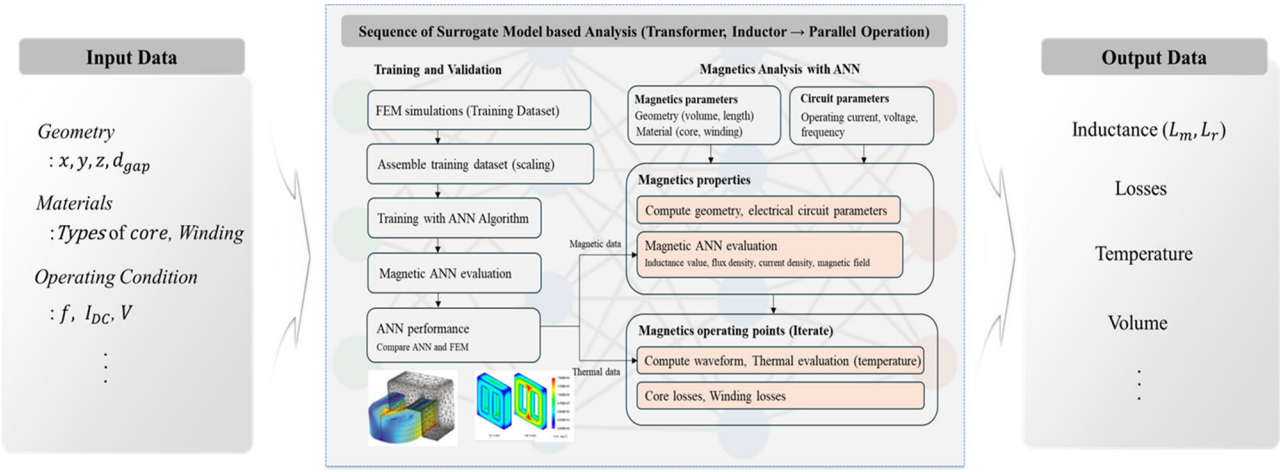

FIGURE 9. AI (Artificial Intelligence) based analysis model for LLC resonant converter.

The conduction loss is calculated by multiplying the resistance magnitude by the rms and average values of the current in the circuit derived through TDA, and can be expressed as (21).

$$P_{con} = 2(\frac{I_{Lr,rms}}{\sqrt{2}})^2 r_{ds(on)1} + (I_{Lr,rms})^2 r_{Cr} + (I_{Lr,rms})^2 r_{Lr} + (I_{Lr,rms})^2 r_{\Pr i} + (I_{\sec,rms})^2 r_{Sec} + 4(I_{\sec,avg} V_F) + 4(\frac{I_{\sec,rms}}{\sqrt{2}})^2 r_F + (\frac{I_{\sec,rms}}{\sqrt{2}})^2 r_{Co} \quad (21)$$

2) THERMAL IMPEDANCE MODEL

Thermal Impedance modeling is a method to estimate the temperature of switches and diodes through the magnitude of loss derived based on TDA, and can express the temperature values of the switch junction and heat sink through a linear relationship with thermal resistance. If the sum of conduction loss and switching loss obtained through the TDA method is defined as P_{sw_Loss}, it can be expressed as (22).

$$P_{sw\_Loss} = P_{Con} + P_{sw} \quad (22)$$

Fig. 8 (a) shows the structure of a switch with a heat sink attached, where the ambient temperature is defined as $T_{ambient}$ and the temperature of the switch junction is defined as $T_{junction}$. The magnitude and temperature of the heat sink's thermal resistance are expressed as R_{Heat} and T_{Heat}, and the magnitude of the thermal resistance of the Thermal Interface Material is represented as R_{TIM}. Additionally, the thermal resistance between the switch junction and case is represented as R_{J-C}, and the temperature of the switch case is expressed as T_{case}. Using this, the thermal resistance equivalent circuit is shown in Fig. 8 (b). In the represented thermal resistance equivalent circuit, the switch's loss is represented as a current source, and the previously defined thermal resistance is represented as a series-connected resistor. At this time, the magnitudes of $T_{Heat}, T_{case}, T_{junction}$ can be expressed through thermal resistance and loss as shown in Equations (19)-(21), respectively.

Through thermal impedance modeling, the junction temperature, case temperature, and heat sink temperature of the switch can be estimated linearly, and through this, temperature information can be estimated.

TABLE 2. Surrogate model input and output variables.

Symbol	Quantity	Type
	Input Variables	
V_{mag}	Magnetics volume	Magnetic, Thermal
A_w	Winding window	Magnetic, Thermal
A_c	Core cross section	Magnetic, Thermal
A_{wc}	Winding and core areas	Magnetic, Thermal
l_{gap}	Air gap length	Magnetic, Thermal
T_a	Ambient temperature	Thermal
h_c	Convection coefficient	Thermal
P_{tot}	Loss per surface	Thermal
P_{mag_Loss}	Winding and core losses	Thermal
r_{sat}	Saturation current	Magnetic
μ_c	Relative core permeability	Magnetic
β_c	Core Steinmetz efficient	Magnetic
	Output Variables	
B	Flux Density	Magnetic
J	Current Density	Magnetic
$Core_{Loss}$	Core Loss	Magnetic
T_{core}	Magnetics Core Temperature	Thermal
T_{wire}	Magnetics Wire Temperature	Thermal

B. AI BASED ANALYSIS MODEL OF MAGNETICS

The AI-based analysis model is a method that generates the relationship between input variables, which are the design variables of magnetic components, and output variables, which are the loss and temperature values of magnetic components, through AI algorithms, and uses this as an analysis model. This analysis model has the advantage of reducing the computational burden compared to simulation-based analysis

models and having higher accuracy compared to mathematical modeling.

$$T_{Heat} = T_{ambient} + P_{sw\_Loss} \cdot R_{Heat} \tag{23}$$

$$T_{case} = T_{ambient} + P_{sw\_Loss} \cdot (R_{Heat} + R_{TIM}) \tag{24}$$

$$T_{junction} = T_{ambient} + P_{sw\_Loss} \cdot (R_{Heat} + R_{TIM} + R_{J-C}) \tag{25}$$

However, tens of input and output variables need to be considered to generate a representative model, and to create an accurate analysis model, it is essential to secure high-quality simulation data and measured values. The input variables for the proposed magnetic analysis model include the shape elements of the magnetic component such as the length, width, height of the core, the length of the gap, the material of the core and winding, and the converter's input and output voltage and operating frequency derived from the circuit analysis. The output variables include the magnetic flux density, current density, loss, temperature, and volume of the magnetic component.

1) TRAINING AND VALIDATION FOR SURROGATE MODEL

Fig. 9 shows the structure of the proposed AI-based analysis model, depicting the flowchart for creating an analysis model based on input and output data [25]. The creation of the analysis model is done in a similar way for both transformers and inductors, and the analysis model built using AI is named the surrogate model. The first step in the process of creating a surrogate model is to generate a dataset using an FEM simulation analysis tool. To create a surrogate model, it is essential to secure a dataset, and in this process, the dataset is created through FEM simulation. At this time, magnetic analysis is performed in analyzing magnetic components, and thermal analysis of the magnetic component is performed based on the loss values obtained through the analysis. The input and output simulation variables needed for the dataset are defined as shown in Table 2. Input variables include $V_{mag,}$ which represents the total volume of the magnetic component, $A_{w,}A_c$ which represent the window area and the cross-sectional area of the core A_{cw}, which is defined as the product of the window area and the core cross-sectional area, the gap length l_g, the ambient temperature $T_{a,}$, the heat convection coefficient $h_{c,}$ the loss magnitude per surface area $P_{tot,}$, the winding loss and core loss $P_{mag\_Loss,}$, the saturation current magnitude $r_{sat,}$, the core material relative permeability $\mu_{c,}$ and the core coefficient β_c. Output variables include the flux density B, current density J, core loss $core_{Loss}$, core temperature T_{core} and wire temperature T_{wire}. Using the simulation results to create an AI-based surrogate model requires scaling work to effectively train the surrogate model. Scaling work is a method of converting data by applying numerical transformations such as proportional constants, logarithmic transformations, or exponential transformations to improve the numerical conditions that each variable has. Normalization is performed based on the scaled data values, and normalization can be performed through the transformation in (22), considering the maximum and minimum values of the corresponding variable.

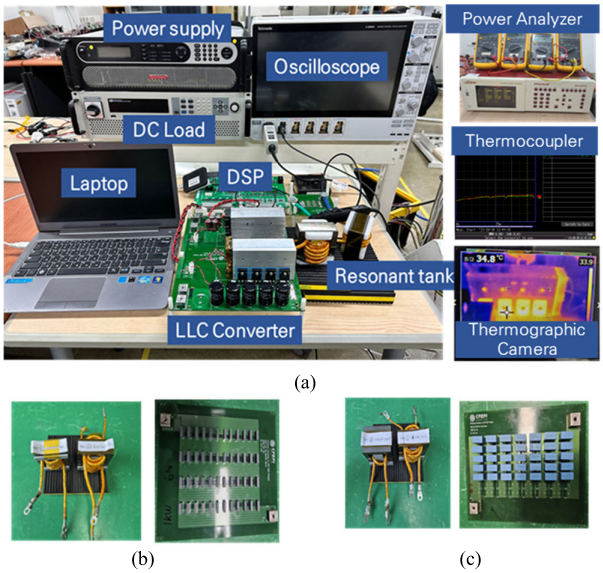

FIGURE 10. Voltage and current waveforms for LLC resonant converter prototype.

The algorithm used for data training to create a surrogate model is the ANN (Artificial Neural Network) technique. The ANN technique is a deep learning technique that mimics the neural network of the human brain, has a multi-layered structure, and neurons in each layer are connected by weights and activation functions. ANN excels at learning and predicting nonlinear problems or complex data patterns, and can achieve high accuracy through learning on large-scale data [39]. The training process of the artificial neural network (ANN) is conducted by dividing the dataset into a training set (80%) and a test set (20%), and the training set is further divided into training and validation subsets. The initial weights and biases of the ANN are randomly selected and are adjusted based on the error indicators obtained through the iterative learning process.

$$x_{nor} = \frac{x - \min(x)}{\max(x) - \min(x)} \tag{26}$$

During the training process, error indicators and indicators for regression result values of the ANN are calculated, and overfitting is continuously calculated. The training process is considered complete when the error indicators converge and improvement stops. Also, if overfitting is detected, the training is stopped, and the error is fed back to prevent performance degradation. The test set, not having been used during training, serves the role of fairly validating the model performance. If the results are not satisfactory, modifications to the ANN structure may be necessary, for example, adjusting the number of hidden layers or neurons.

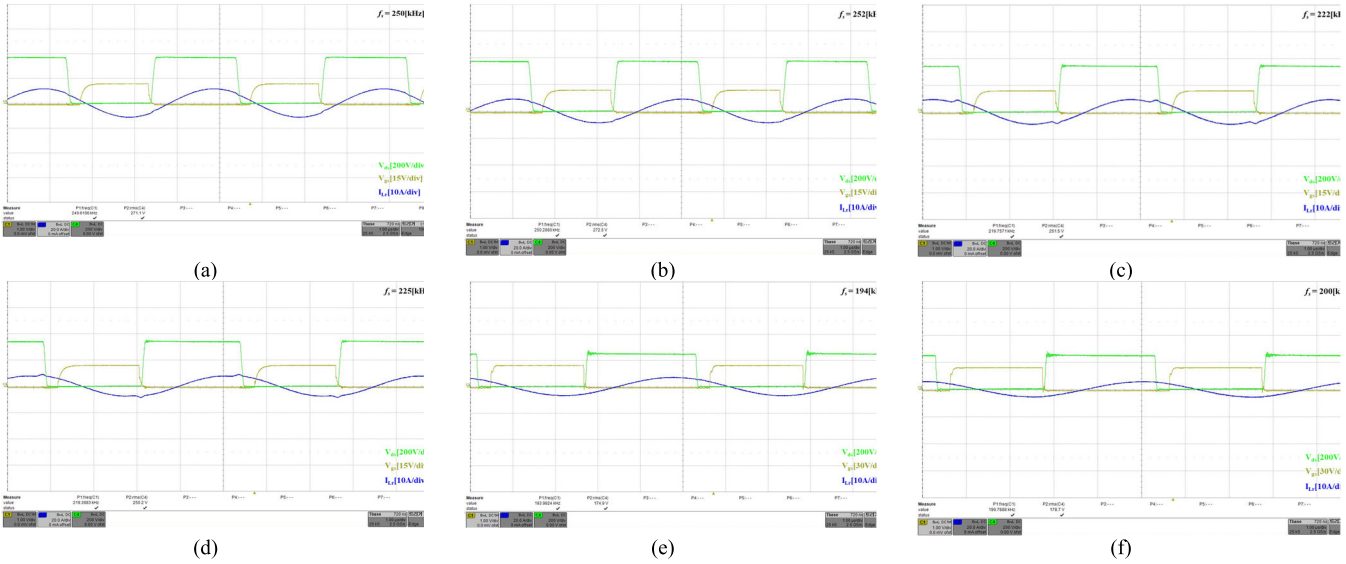

FIGURE 11. Waveforms of current and voltage of the LLC resonant converter Prototype at different cases.

TABLE 3. Parameters of LLC resonant converter.

Symbol	Quantity	Value
P_o	Capacity	150-1000[W]
V_{in}	Input Voltage	240-360[V]
V_{out}	Output Voltage	120-180[V]
	Resonant Tank, Switch, Diode (Type A, B)	
f_r	Resonant Frequency	200-250[kHz]
L_r	Resonant Inductance	6.14-11.5[uH]
C_r	Resonant Capacitance	55-66[nF]
L_m	Magnetic Inductance	21.49-23 [uH]
f_{sw}	Switching Frequency	194-252[kHz]
SW_{type}	Switch Type	TP65H015G5WS/ GAN063-650WSA
D_{type}	Diode Type	SCS230AE2HRE/ MSC030SDA120B
	Heatsink, FAN	
SWH_{type}	Switch Heatsink	20×10×4[mm] (Fin type)
SWF_{type}	Switch FAN	20×10×4[mm] (Fin type)
	Transformer specifications (Type A, B)	
$Core_{TRtype}$	Transformer Core	EE5555/EE 6565
$Core_{TRmat}$	Transformer Material	PM12
$Core_{TRnum}$	Number of Transformer Core	1
$Wire_{TRpri}$	Transformer Primary Wire	0.12[mm]/500,650
$Wire_{TRsec}$	Transformer Secondary Wire	0.12[mm]/1200
l_{TRg}	Transformer Air gap	0.08-0.11[cm]
N_{TRp}	Transformer Primary Turns	6-9[Turns]
N_{TRs}	Transformer Secondary Turns	5-8[Turns]
	Inductor specifications (Type A, B)	
$Core_{Indtype}$	Inductor Core	EE5555/EE 6565
$Core_{Indmat}$	Inductor Material	PM12
$Core_{Indnum}$	Number of Inductor Core	1
$Wire_{Ind}$	Inductor Wire	0.12[mm]/500
l_{Indg}	Inductor Air gap	0.11-0.14[cm]
N_{Ind}	Inductor Turns	7-9[Turns]

TABLE 4. Experimental specifications for different cases.

Case	Capacity	Input Voltage	Output Voltage	Switch & Diode	Resonant Tank
(a)	1000[W]	360	180	Type A	Type A
(b)	600[W]	360	180	Type A	Type A
(c)	600[W]	330	180	Type B	Type A
(d)	300[W]	330	180	Type B	Type A
(e)	300[W]	240	120	Type A	Type B
(f)	150[W]	240	120	Type B	Type B

2) MAGNETIC ANALYSIS WITH SURROGATE MODEL

The magnetic components are analyzed using the transformer and inductor magnetic and thermal surrogate models derived through the training process described earlier. When magnetic shape parameters such as the volume and length of the magnetic component, parameters such as the core and winding material, and circuit analysis parameters such as operating voltage, current, and frequency are applied to the surrogate model, magnetic characteristics (e.g., inductance, saturation current, magnetic and thermal field patterns) are extracted. In this process, designs that do not meet the specifications are filtered out.

At this time, core loss is calculated using detailed loss data considering the effects of frequency, AC flux density, DC flux density, and temperature. Winding loss is calculated including the effects of proximity loss and harmonics. Temperature is evaluated through a thermal model considering the magnitude of loss. Data is repeatedly exchanged between the loss model and the thermal model to reach a steady state (coupled loss-thermal model) for the values. Similarly, designs that do not meet specifications or have poor performance are filtered out to maintain the performance of the analysis model at a certain level or above.

Through this, results such as core and winding loss, core and winding temperature, volume, etc., can be derived.

IV. PERFORMANCE VERIFICATION

To verify the performance of the proposed analysis model, a prototype of the LLC resonant converter was designed and

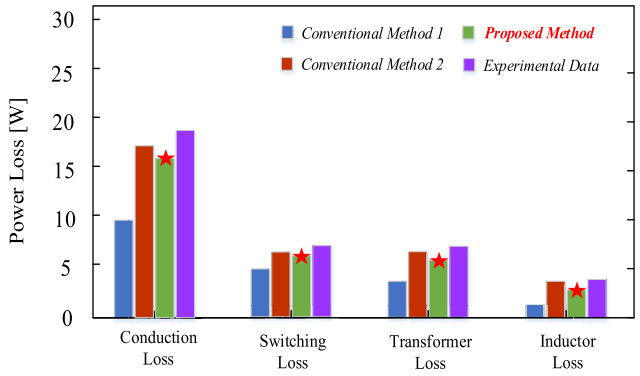

FIGURE 12. The comparison of loss breakdown between different method.

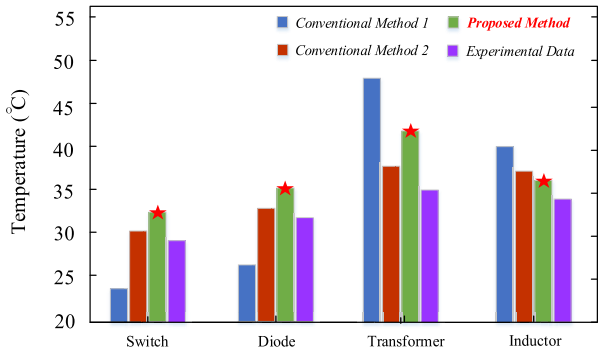

FIGURE 13. The comparison of temperature estimation between different method.

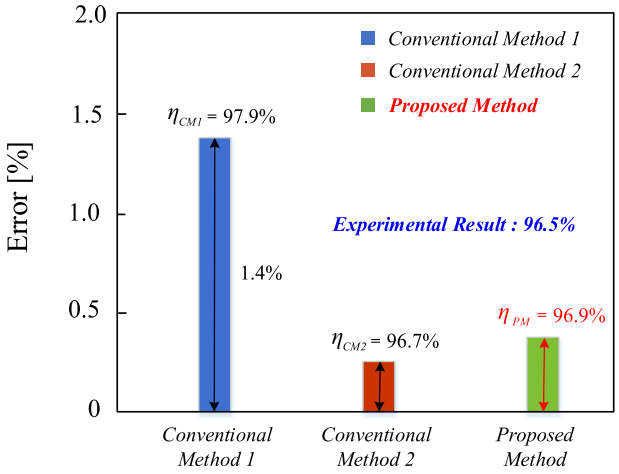

FIGURE 14. The comparison of efficiency estimation error between different method.

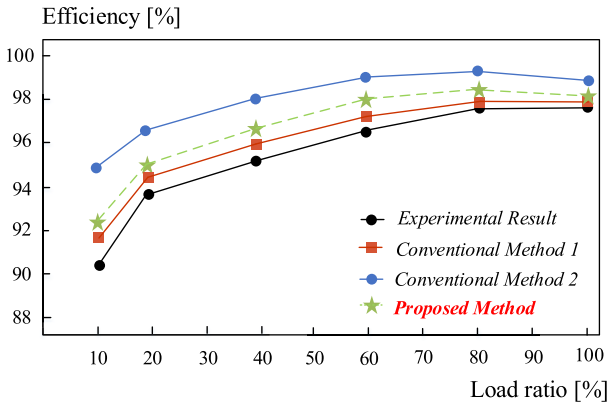

FIGURE 15. The comparison of efficiency estimation according to load ratio between different method.

manufactured. Fig. 10 (a) shows the verification environment, consisting of an LLC resonant converter prototype, a DC amplifier for input, output voltage, and load, and an oscilloscope for waveform measurement. Additionally, a power meter for measuring efficiency and a digital multimeter for measuring precise DC voltage and current values were used. For temperature, to increase the accuracy of measurement, a temperature point meter and a thermal imaging camera were used to measure the temperature of switches, diodes, inductors, and transformers. To broadly verify the reliability of the proposed analysis model, verification was conducted under various input, output voltage, load rate, switch, and resonant network conditions, and the parameters are shown in Table 3.

The capacity of the converter prototype is 1000W, and input voltage ranges from 240V to 360V, and output voltage from 120V to 180V. The resonant frequency is designed to be 200kHz-250kHz, the resonant inductance is set to 6.14-11.5[uH], the resonant capacitance to 21.49-23[nF], and the magnetizing inductance to 55-66[uH]. The switching frequency is adjusted according to the input, output voltage, and load magnitude, and is controlled to output a constant output voltage within the range of 194-250[kHz]. Two types of Lead-type GaN-based switches (Type A, B) are used, with Type A being Transphorm's TP65H015G5WS and Type B being Nexperia's GAN063-650WSA. Similarly, two types of diodes are used, with Type A using Rohm's SCS230AE2HR diode and Type B using Microsemi's MSC030SDA120B. The heat sink for switches and diodes uses a pin-type heat sink of 20 × 10×4[mm], and the fan used is CUI CFM-25B. The resonant network design is mainly carried out in two types, with the first Type A having a resonant inductance of 6.14[uH], a magnetizing inductance of 21.49[uH], and a resonant capacitor of 66[nF] based on a resonant frequency of 200[kHz]. The core used for the transformer design among magnetic components is EE6565, the core material is PM12, and the number of cores used is 1. The wiring used is 0.12[mm]/500 for the primary side and 0.12[mm]/1200 for the secondary side winding, and the gap length is 0.11[cm], and the number of turns for the primary and secondary sides is designed as 9 turns and 8 turns, respectively. For the inductor, EE5555 is used, the material is PM12, and the number of cores used is 1. The wire used is 0.12[mm]/500, and the gap length is 0.1426[cm]. The number of turns is designed as 9 turns. The prototype is shown in Fig. 10 (b). Type B resonant network has a resonant frequency of 250[kHz], a resonant inductance of 11.5[uH], a magnetizing inductance of 23[uH],

and a resonant capacitor of 55[nF]. The core used for the transformer design among magnetic components is EE5555, the core material is PM12, and the number of cores used is 1. The wiring used is 0.12[mm]/500 for the primary side and 0.12[mm]/1200 for the secondary side winding. The gap length is 0.08[cm], and the required number of turns for the primary and secondary sides is designed as 6 turns and 5 turns. For the inductor, EE6565 is used, the material is PM12, and the number of cores used is 1. The wire used is 0.12[mm]/500, the gap length is 0.14[cm], and the number of turns is designed as 7 turns. The prototype is shown in Fig. 10 (c). Fig. 11 shows the waveforms representing the operation of the LLC resonant converter under various operating conditions according to the resonant network candidates and the types of switches and diodes. The drain-source voltage, gate-source voltage, and resonant current magnitude of the lower switch of the HB-type LLC resonant converter were measured. Waveforms were measured based on 6 representative test cases, and through the adjustment of dead time, it can be seen that zero-voltage switching is performed as the gate waveform operates after the drain-source voltage drops to 0. Specifically, the operating condition in Fig. 11(a) is 1kW, and input and output voltages of 360[v] and 180[v], respectively. At this time, Type A was used for both the switch and diode, and Type A was used for the resonant network. The effectiveness of the proposed analysis model was verified through verification under the operating conditions corresponding to Fig. 11 (b)-(f) and the types of diodes and passive elements. Fig. 12 shows the magnitude of conduction loss, switching loss, and magnetic loss of the LLC resonant converter under the case (a) verification condition, comparing the performance of conventional methods and the proposed method against experimental measured values. For the first conventional method, a mathematical modeling-based analysis model is considered, using the FHA technique for circuit analysis, the IGSE technique for magnetic loss analysis, and a temperature analysis formula based on experimental formula for temperature. For the second conventional method, a simulation-based analysis model is considered, using professional circuit analysis tools such as PSIM and PLECS for circuit analysis, and FEM-based simulation for magnetic loss and temperature analysis. For conduction loss, when the loss magnitude was derived based on measured values, it was 18.3[W], and the proposed method estimated the conduction loss magnitude as 15.5[W]. The first conventional method based on mathematical modeling estimated it as 9.5[W], and the second conventional method based on simulation estimated it as 17[W]. Similarly, for switching loss, transformer loss, and inductor loss, it can be seen that the accuracy of the proposed method is higher than that of the first conventional method based on mathematical modeling and lower than that of the second conventional method based on simulation. Fig. 13 shows the magnitude of the LLC resonant converter's switch temperature, diode temperature, and magnetic component temperature under the case (a), comparing the performance of conventional methods and the proposed method against experimental measured values. The specifications are summarized in Table 4, and verification was conducted through various capacity condition, input and output voltages, and switch specifications. At this time, the temperature of switches and diodes was measured and calculated based on the heat sink temperature of the components, and the temperature of the transformer and inductor was measured and calculated based on the temperature of the core and wire. The results mainly summarize the measurement and calculation data for the core temperature of magnetic components, and the temperature values were recorded based on values that did not change by more than 3 degrees during 10 minutes. The first conventional method uses a mathematical modeling-based analysis model, using thermal impedance-based modeling method to determine the temperature of switches and diodes, and using an experimental formula based on experimental data for the temperature of magnetic components. The second conventional method based on mathematical modeling performed thermal analysis and magnetic analysis based on FEM, and derived values based on the results obtained through magnetic and thermal analysis simulations. In the case of switches, the measured temperature under case (a) was 28.3 degrees, and the first conventional method estimated the value as 23 degrees. The second conventional method estimated the temperature as 30 degrees, and the proposed method estimated it as 33 degrees. Diodes also showed a similar trend compared to the measured value as switches, and it can be seen that the temperature estimation error of the proposed method is within 5 degrees. For magnetic components, the measured temperature of the transformer was 35 degrees, and the estimated temperature in the first conventional method was 47.2 degrees, while the second conventional method estimated it as 38.1 degrees. The proposed method estimated it as 41.7 degrees, showing that the error from the measured value is within 7 degrees. In the case of inductors, they showed a similar trend as transformers, with the measured value being 25.8 degrees, and the proposed method estimating it as 29.2 degrees, confirming that the temperature was estimated with an error of about 3-4 degrees. The proposed method adopts a hybrid approach that combines a time-domain mathematical model with an AI-based analysis model. This approach achieves a balance by significantly reducing the computational burden compared to conventional method 2 which uses simulation for analysis of LLC converter, while maintaining sufficient estimation accuracy. As shown in Figures 12 and 13, simulation-based methods may offer slightly higher estimation accuracy under certain conditions. However, the proposed method exhibits a substantial improvement in computational efficiency, which greatly enhances its practicality and applicability in design of the LLC Converter. Fig. 14 is a graph comparing the efficiency estimation error of the LLC resonant converter under the same verification condition. The measured efficiency under case (a) condition is 96.5%. At this time, the first conventional method has an estimated efficiency of 97.9%,

showing a 1.4% estimation error compared to the measured efficiency, and the second conventional method has 96.7%, showing a 0.2% estimation error compared to the measured efficiency. The estimated efficiency of the proposed method is 96.9%, showing a 0.4% estimation error compared to the measured efficiency. Through this, it can be seen that the proposed method has a higher accuracy compared to the first conventional method and does not have a large difference from the measured efficiency value. Fig. 15 is a graph showing the magnitude of resonant converter efficiency according to the load magnitude under the case (a). The graph analyzed in Fig. 12-14 earlier shows the magnitude of losses by type, temperature, and efficiency of the LLC resonant converter at 100% load, and the estimation accuracy by analysis model according to the load magnitude was confirmed. This graph shows the efficiency estimation accuracy by analysis model according to the load rate, and it can be seen that the efficiency estimation accuracy of the first conventional method decreases significantly as it goes to light loads. It can be confirmed that the first conventional method has a maximum estimation error of within 5% at 10-20% load rate. In the case of the first conventional method, the estimation accuracy varies depending on the load rate, and due to this, it can be seen that the estimation accuracy at light loads is low. In contrast, it can be seen that the second conventional method estimates efficiency with high accuracy even at low load rates, and the maximum estimation error at 10-20% load rate is about 1%. The proposed method has an efficiency estimation error of about 2% at 10-20% load rate. Through this, it can be seen that the proposed method estimates efficiency with relatively high accuracy even from the perspective of load rate. Fig. 16 shows the efficiency estimation accuracy according to the case, and when changing various conditions such as switch, diode, and resonant network design values, it can be seen that the first conventional method has an error of 4-5%, and the second conventional method has an error of about 1%. In the case of the proposed method, it can be seen that it estimates efficiency with an error of about 2%. Through this, the efficiency estimation accuracy of the proposed method was verified under various conditions, and it can be seen that it estimates the efficiency of the LLC resonant converter within 2%. Fig. 17 is a graph comparing the computation time by technique. The computational burden and time refers to the total time required to analyze the LLC resonant converter. The proposed method combines an improved time-domain analysis (TDA) model and an AI-based magnetic component analysis model. The computation time of the TDA model for circuit analysis is defined as the time required from inputting the operating parameters to obtaining the estimated loss and efficiency values. For magnetic component analysis, based on this trained black-box model, the analysis is performed by inputting the required parameters and extracting the corresponding outputs. The computation time is defined as the time taken from parameter input to the generation of outputs such as temperature, loss, and volume. Therefore, the overall computation time of the proposed hybrid analysis model includes the computation time for TDA-based circuit analysis, the computation time for AI-based magnetic component analysis, and the time required for mutual information exchange between the two for total analysis of LLC converter. This total time reflects the full process of estimating key performance metrics such as efficiency and temperature of the LLC resonant converter. In the case of the first conventional method, since it uses a mathematical modeling-based analysis formula, it can immediately obtain values such as efficiency and temperature when the design and analysis conditions of the LLC resonant converter are given. The second conventional method is a simulation-based analysis method, and since it derives result values through circuit and magnetic simulations, it takes relatively more time, and the difference in computation time varies greatly depending on the accuracy of the analysis. The required time is 650[s], which is the time required when performing calculations based on a CPU i7 core. Generally, the time required to derive simulations varies depending on the complexity of the model. The second conventional method used in this verification performed the analysis based on an ideal magnetic FEM model with not high model complexity and derived values under the minimum analysis environment (basic mesh number and Time step). meaningful analysis results using FEM and circuit. Also, in the case of circuit simulation, the required computation time varies depending on the time step in the simulation itself and the accuracy of the model, and to secure normal performance, a computation time of at least 60[s] to as long as tens of minutes is typically needed. The simulation performed similar to the magnetic analysis with the model complexity not being high, and since the circuit and magnetic analysis simulations are performed in parallel, the computation time was measured based on the computation time of the magnetic analysis, which requires a bit more computation time. Fig. 18 is a graph showing the computation time according to the increase in the number of analyses. Not only for accurate analysis of the LLC resonant converter but also for effective optimal design ultimately, several design candidates need to be considered, and accurate analysis of each design candidate is required. Therefore, an analysis model that can accurately analyze several design candidates in not too long a time is needed, and if the required analysis time and computational burden are large, the number of candidates that can be considered may be limited, making it difficult to derive effective optimal design values. The first existing method uses a mathematical modeling-based analysis formula, so there is not a large computational burden when performing analyses according to different design and analysis specifications. In contrast, the second conventional method requires 650[s] of analysis time for one design condition and specification, so for 100 analyses, about 65000[s] is required, necessitating computation within 18 hours. The proposed method takes about 70[s] for one analysis, so for 100 analyses, the analysis time is 7000[s], requiring time within 2 hours. Since the design variables of the LLC resonant converter are diverse, for complex analysis considering the interrelationship of each

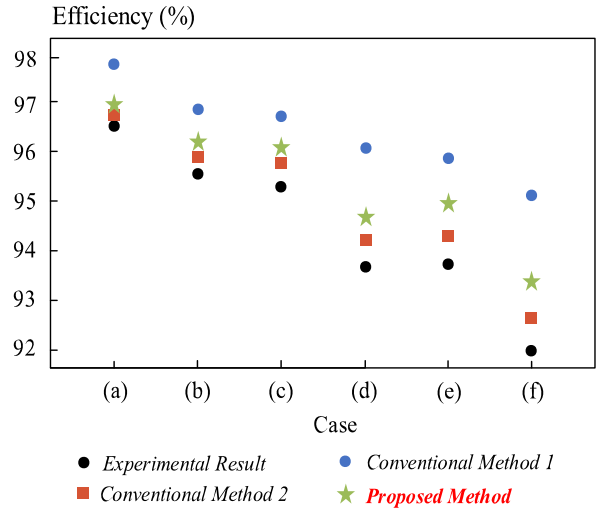

FIGURE 16. The comparison of efficiency estimation for different cases between different method.

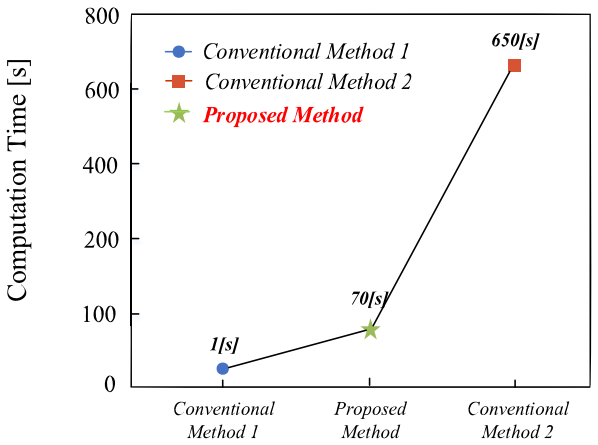

FIGURE 17. The comparison of computation time between different method.

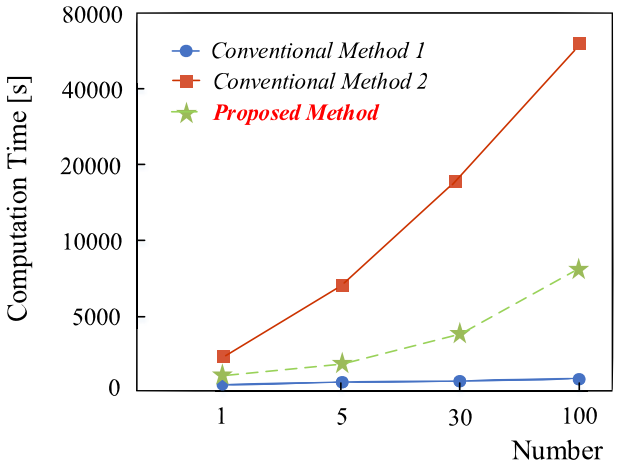

FIGURE 18. The comparison of computation time according to analysis number between different method.

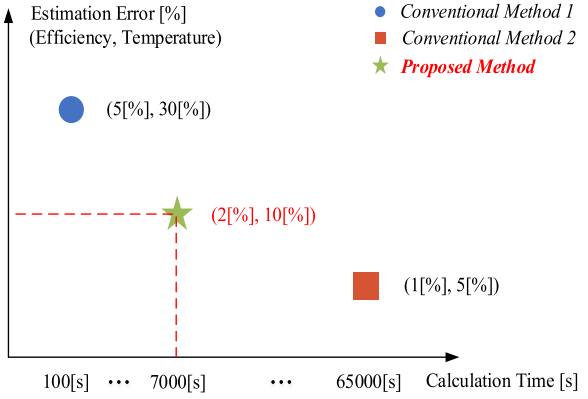

FIGURE 19. The comparison of computation time and estimation error between different method.

design variable and further comprehensive optimal design, analyses need to be performed multiple times, and for this, the number of analysis candidates can increase even more. At this time, the difference in required computation time by each technique increases exponentially. Fig. 19 is a graph that reflects the efficiency, temperature estimation accuracy, and computation time of conventional methods in one graph. The estimation error is indicated based on the worst case according to the verification condition and load rate. In the case of the first conventional method, the efficiency estimation error is about 5[%], and the temperature estimation error is about 40[%]. When considering 100 analyses, the required computation time is 100[s]. In the case of the second conventional method, the efficiency estimation error is about 1%, and the temperature estimation error is about 5[%]. When considering the same number of analyses, the required computation time is 65000[s]. The efficiency estimation error of the proposed method is about 2[%], and the temperature estimation error is 10[%]. When considering the same number of analyses, the required computation time is 7000[s]. Through this, it can be seen that the proposed method is a method that can secure efficiency and temperature estimation accuracy performance while also reducing the computational burden.

V. CONCLUSION

An efficient analysis model with high accuracy while not requiring a large computational burden was proposed for analyzing LLC resonant converters. The proposed model adopts and uses a Hybrid form of analysis model that combines an advanced mathematical modeling-based circuit and temperature analysis model with an AI-based magnetic analysis model. Through the TDA-based analysis method, circuit analysis is performed to derive the voltage and current magnitude in the circuit with high accuracy, and through this, the loss of switches and diodes can be determined. Based on the derived loss values, the temperature values of switches and diodes are determined through a

thermal impedance model. For magnetic analysis, a representative model is built by training FEM simulation data using the ANN algorithm, and through this, the magnitude of loss and temperature of magnetic components is calculated.

The proposed method was compared with two existing analysis models, and the accuracy of efficiency and temperature estimation was measured under various capacity, input and output voltage, resonant network value, and load conditions. In the case of the first conventional method based on mathematical modeling, the efficiency and temperature estimation errors were about 5[%] and 30[%], respectively, and the efficiency and temperature estimation errors of the second conventional method based on simulation were 1[%] and 5[%], respectively. The efficiency and temperature estimation errors of the proposed method are 2[%] and 10[%], respectively. At this time, the computation time required for the analysis model is 100[s] for the first technique, 65000[s] for the second conventional method, and 7000[s] for the proposed method based on 100 analyses, showing a low computational burden. Through this, it was confirmed that the proposed method can effectively analyze LLC resonant converters with high accuracy and relatively low computational burden compared to conventional methods. This method can perform effective review of various design variables and specifications of LLC resonant converters, and the effect of the proposed method can be expected to increase when optimally designing converters.

REFERENCES

[1] C. Wang, M. Li, Z. Ouyang, T.-G. Zsurzsan, and M. A. E. Andersen, "Pentacentra transformer for multiphase LLC converter in high-current data center application," *IEEE Trans. Power Electron.*, vol. 39, no. 1, pp. 1150–1161, Jan. 2024.

[2] I. Khan, S. Rahman, M. A. Ayaz, M. Amir, and H. Shehada, "Review of isolated DC–DC converters for application in data center power delivery," *IEEE Trans. Ind. Appl.*, vol. 60, no. 4, pp. 5436–5446, Jul. 2024.

[3] J.-Y. Lin, H.-Y. Yueh, Y.-F. Lin, and P.-H. Liu, "Variable-frequency and phase-shift with synchronous rectification advance on-time hybrid control of LLC resonant converter for electric vehicles charger," *IEEE J. Emerg. Sel. Topics Ind. Electron.*, vol. 4, no. 1, pp. 348–356, Jan. 2023.

[4] S. Ding, C. Nie, Q. Liu, Q. Qian, and W. Sun, "High efficiency high power density bidirectional non-isolated LLC converter with transformer-coupled gate driver for 48 v MHEV," *IEEE Open J. Power Electron.*, vol. 6, pp. 747–760, 2025.

[5] Y. Li, J. Bao, B. Liu, and S. Duan, "Design and optimization of vertically integrated four-leg matrix transformer for bidirectional LLC converter," *IEEE Trans. Ind. Electron.*, vol. 72, no. 4, pp. 3840–3850, Apr. 2025.

[6] J. Wang, J. Hu, W. Pei, Z. Yang, J. Zhuang, and X. Zhang, "In-depth design and multiobjective optimization of an integrated transformer for five-phase LLC resonant converters," *IEEE Trans. Power Electron.*, vol. 37, no. 11, pp. 13538–13553, Nov. 2022.

[7] B. Yang, F. C. Lee, A. J. Zhang, and G. Huang, "LLC resonant converter for front end DC/DC conversion," in *Proc. APEC. 17th Annu. IEEE Appl. Power Electron. Conf. Expo.*, vol. 2, Mar. 2002, pp. 1108–1112.

[8] J. Deng, S. Li, S. Hu, C. C. Mi, and R. Ma, "Design methodology of LLC resonant converters for electric vehicle battery chargers," *IEEE Trans. Veh. Technol.*, vol. 63, no. 4, pp. 1581–1592, May 2014.

[9] S. De Simone, C. Adragna, C. Spini, and G. Gattavari, "Design-oriented steady-state analysis of LLC resonant converters based on FHA," in *Proc. Int. Symp. Power Electron., Electr. Drives, Autom. Motion (SPEEDAM)*, Taormina, Italy, 2006, pp. 200–207.

[10] Y. Wei, T. Pereira, Y. Pan, M. Liserre, F. Blaabjerg, and H. A. Mantooth, "A general and automatic RMS current oriented optimal design tool for LLC resonant converters," *IEEE J. Emerg. Sel. Topics Power Electron.*, vol. 10, no. 6, pp. 7318–7332, Dec. 2022.

[11] Y. Wei, Q. Luo, and A. Mantooth, "Comprehensive comparisons between frequency-domain analysis and time-domain analysis for LLC resonant converter," *IET Power Electron.*, vol. 13, no. 9, pp. 1735–1745, Jul. 2020.

[12] J. Niu, Y. Tong, Q. Ding, X. Wu, X. Xin, and X. Wang, "Time domain simplified equations and its iterative calculation model for LLC resonant converter," *IEEE Access*, vol. 8, pp. 151195–151207, 2020.

[13] H. Wouters and W. Martinez, "Integrated inductor-transformers for high-frequency converters: An overview," *IEEE Trans. Power Electron.*, vol. 40, no. 9, pp. 13157–13176, Sep. 2025.

[14] Z. Li, W. Han, Z. Xin, Q. Liu, J. Chen, and P. C. Loh, "A review of magnetic core materials, core loss modeling and measurements in high-power high-frequency transformers," *CPSS Trans. Power Electron. Appl.*, vol. 7, no. 4, pp. 359–373, Dec. 2022.

[15] *LED Application Design Guide Using Half-Bridge LLC Resonant Converter for 100W Street Lighting*, document AN-9729, Rev 1., Fairchild Semiconductor Corporation, 2012.

[16] H. Huang, "Designing an LLC resonant half-bridge power converter," in *Texas Instruments Power Supply Design Seminar*, 2010, pp. 1–27.

[17] Y. Wei, Q. Luo, X. Du, N. Altin, J. M. Alonso, and H. A. Mantooth, "Analysis and design of the LLC resonant converter with variable inductor control based on time-domain analysis," *IEEE Trans. Ind. Electron.*, vol. 67, no. 7, pp. 5432–5443, Jul. 2020.

[18] C. Ma, X. Zhu, Z. Chen, and B. Zhang, "Time domain analysis and gain curve modeling of fractional-order full-bridge LLC resonant converter," *IEEE Trans. Power Electron.*, vol. 40, no. 9, pp. 13035–13049, Sep. 2025.

[19] J. Jiao, X. Guo, C. Wang, and X. You, "Time-domain analysis and optimal design of LLC-DC transformers (LLC-DCXs) considering discontinuous conduction modes," *IEEE Trans. Transport. Electrific.*, vol. 9, no. 2, pp. 2308–2323, Jun. 2023.

[20] M. J. Jacoboski, A. de Bastiani Lange, and M. L. Heldwein, "Closed-form solution for core loss calculation in single-phase bridgeless PFC rectifiers based on the iGSE method," *IEEE Trans. Power Electron.*, vol. 33, no. 6, pp. 4599–4604, Jun. 2018.

[21] J. Kolar, J. Biela, and J. Minibock, "Exploring the Pareto front of multi-objective single-phase PFC rectifier design optimization–99.2% efficiency vs. 7kW/din3 power density," in *Proc. IEEE 6th Int. Power Electron. Motion Control Conf.*, May 2009, pp. 1–21.

[22] T. Wang and J. Yuan, "Improvement on loss separation method for core loss calculation under high-frequency sinusoidal and non-sinusoidal excitation," *IEEE Trans. Magn.*, vol. 58, no. 8, pp. 1–9, Aug. 2022.

[23] V. Bertolini, M. Stella, and R. Scorretti, "Circuit modelling of static magnetic losses of ferrite cores and application on an LLC converter," in *Proc. IEEE EUROCON 20th Int. Conf. Smart Technol.*, Jul. 2023, pp. 429–433.

[24] S. Rajur, S. Bhat, V. Kulkarni, A. Laddigatti, and V. Muratti, "Design and operation of resonant LLC converter for EV applications using PLECS simulation," in *Proc. Int. Conf. Ambient Intell., Knowl. Informat. Ind. Electron. (AIKIIE)*, Ballari, India, Nov. 2023, pp. 1–4.

[25] T. Guillod, "Modeling and design of medium-frequency transformers for future medium-voltage power electronics interfaces," Ph.D. dissertation, ETH Zürich, 2018.

[26] T. Guillod, P. Papamanolis, and J. W. Kolar, "Artificial neural network (ANN) based fast and accurate inductor modeling and design," *IEEE Open J. Power Electron.*, vol. 1, pp. 284–299, 2020.

[27] S. Subedi, Y. Gui, and Y. Xue, "Applications of data-driven dynamic modeling of power converters in power systems: An overview," *IEEE Trans. Ind. Appl.*, vol. 61, no. 2, pp. 2434–2456, Mar. 2025.

[28] S. Reese, B. Sauter, and D. Maksimović, "Data-driven component-level design of switching power converters using predictive modeling," *IEEE Trans. Power Electron.*, vol. 40, no. 8, pp. 11126–11142, Aug. 2025.
[29] J.-H. Jung and J.-G. Kwon, "Theoretical analysis and optimal design of LLC resonant converter," in *Proc. Eur. Conf. Power Electron. Appl.*, Aalborg, Denmark, 2007, pp. 1–10.
[30] C. P. Steinmetz, "On the law of hysteresis," *Proc. IEEE*, vol. 72, no. 2, pp. 197–221, Feb. 1984.
[31] J. Reinert, A. Brockmeyer, and R. W. A. A. De Doncker, "Calculation of losses in ferro- and ferrimagnetic materials based on the modified steinmetz equation," *IEEE Trans. Ind. Appl.*, vol. 37, no. 4, pp. 1055–1061, 2001.
[32] J. Li, T. Abdallah, and C. R. Sullivan, "Improved calculation of core loss with nonsinusoidal waveforms," in *Proc. Conf. Rec. IEEE Ind. Appl. Conf. 36th IAS Annu. Meeting*, vol. 4, 2001, pp. 2203–2210.
[33] K. Venkatachalam, C. R. Sullivan, T. Abdallah, and H. Tacca, "Accurate prediction of ferrite core loss with nonsinusoidal waveforms using only steinmetz parameters," in *Proc. IEEE Workshop Comput. Power Electron.*, Jun. 2002, pp. 36–41.
[34] D. Ahmed, L. Wang, Z. Dai, and M. Wu, "Pareto-optimal design of litz-wire gapped-core high-frequency transformer for LLC converters," *IEEE Trans. Ind. Electron.*, vol. 69, no. 9, pp. 8883–8894, Sep. 2022.
[35] X. Dexin, T. Yunqiu, and X. Zihong, "FEM analysis of 3D eddy current field in power transformer," *IEEE Trans. Magn.*, vol. MAG-23, no. 5, pp. 3786–3788, Sep. 1987.
[36] K. Preis, O. Biro, and G. Buchgraber, "Thermal-electromagnetic coupling in the finite-element simulation of power transformers," *IEEE Trans. Magn.*, vol. 42, no. 4, pp. 999–1002, Apr. 2006.
[37] E. S. Glitz and M. Ordonez, "MOSFET power loss estimation in LLC resonant converters: Time interval analysis," *IEEE Trans. Power Electron.*, vol. 34, no. 12, pp. 11964–11980, Dec. 2019.
[38] Y. Wei, Z. Wang, Q. Luo, and H. A. Mantooth, "MATLAB GUI based steady state open-loop and closed-loop simulation tools for different LLC converters with all operation modes," *IEEE Open J. Ind. Appl.*, vol. 2, pp. 320–336, 2021.
[39] S.-S. Park, M.-H. Eom, S.-T. Lee, and R.-Y. Kim, "Accurate analysis method and voltage gain curve derivation algorithm based on time-domain analysis for high-efficiency LLC resonant converter design," *Electronics*, vol. 12, no. 9, p. 2030, Apr. 2023.
[40] O. I. Abiodun, A. Jantan, A. E. Omolara, K. V. Dada, A. M. Umar, O. U. Linus, H. Arshad, A. A. Kazaure, U. Gana, and M. U. Kiru, "Comprehensive review of artificial neural network applications to pattern recognition," *IEEE Access*, vol. 7, pp. 158820–158846, 2019.

SU-SEONG PARK received the B.S. degree in electrical engineering and the Ph.D. degree from Hanyang University, Seoul, South Korea, in 2020 and 2025, respectively. He has been a Postdoctoral Researcher with the Department of Energy and Electrical Engineering, Hanyang University. His research interests include the design of high-density, high-efficiency power converters, the control of distributed power converter systems, renewable energy, microgrids, HVDC, STATCOM, and FACTS systems.

RAE-YOUNG KIM (Senior Member, IEEE) received the B.S. and M.S. degrees from Hanyang University, Seoul, South Korea, in 1997 and 1999, respectively, and the Ph.D. degree from Virginia Polytechnic Institute and State University, Blacksburg, VA, USA, in 2009, all in electrical engineering.

From 1999 to 2004, he was a Senior Researcher with the Hyosung Heavy Industry Research and Development Center, Seoul. In 2009, he was a Postdoctoral Researcher at National Semiconductor Corporation, Santa Clara, CA, USA, involved in a smart home energy management system. In 2016, he was a Visiting Scholar at the Center for Power Electronics Systems (CPES), Virginia Polytechnic Institute, and State University, Blacksburg. Since 2010, he has been with Hanyang University, where he is currently a Professor at the Department of Electrical and Biomedical Engineering. His research interests include the design of high-power density converters and the distributed control of power converters for modular power converter systems in applications of renewable energy, wireless power transfer, microgrids, and motor drives.

Dr. Kim was a recipient of the 2007 First Prize Paper Award from IEEE IAS.